Size Controlled Nanogels

DEVELOPMENT OF SIZE CONTROLLED NANOGELS FOR BIOMEDICAL APPLICATIONS

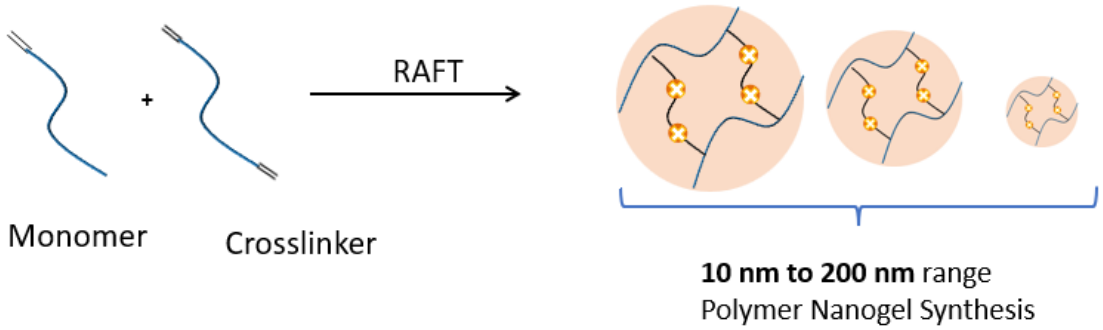

B.L.H. Kleinlugtenbeld (S2242680) – BSc Biomedical Technology – University of Twente

Date of publication: 5-7-2022

N. Cengiz PHD (daily supervisor)

Dr.Ir. J.M.J. Paulusse (supervisor)

Prof. Dr. J.J.L.M. Cornelissen (chair member)

Dr. A.S.Y. Wong (external member)

Abstract

In this thesis, it is aimed to make size controlled nanogels. For the fabrication of nanogels, functional methacrylate monomers will be used together with dimethacrylate crosslinkers in a ratio 3:1, utilizing the RAFT (Reversible-addition-fragmentation chain-transfer) technique. This technique promotes the formation of uniform particles with a low polydispersity in a controlled manner and is also applicable to various monomers. Size-controlled nanogels might be the future for serving as a biomedical application. During the synthesis of the nanogels, a size range of 8-146 nm was achieved. However, more data points are required to make it a more reliable range. These synthesis of nanogels were characterised through the use of NMR, DLS, GPC.

Table of content

1. Introduction

1.1 Nanogel Applications

In recent years nanogels have been intensively investigated for their various biomedical applications, such as drug delivery, gene therapy, tissue engineering and imaging[1]. Nanogels are three-dimensional hydrogel materials[2] in the nanoscale size range formed by crosslinked polymers. These nanogels possess softness, biocompability and water uptake capacity. On the other hand, nanogels have the ability to encapsulate guest molecules[3]. Due to these properties nanogels can be used for surface coating, drug delivery and imaging agents[4,5].

As mentioned above, nanogels can be used for various biomedical applications. One of these biomedical application is the function as a drug delivery system through the human body[1]. There are several areas in the body where it is difficult for drugs to enter, such as the blood brain barrier[6]. Due to some of these biological barriers in the body, multiple lifesaving drugs cannot get through and cure diseases as HIV-1 encephalitis, Alzheimer's disease, ischemia, tumours, multiple sclerosis, and Parkinson's disease[7]. Nanogels might give a solution for getting drugs to enter protected areas.

When looking at distribution studies of nanomaterial in general, the size plays a major role. Particles of < 200 nm have been reported to be taken up into the spleen, while particles below 70 nm are mostly found in the liver[8,9]. Furthermore, literature shows examples of particles with a size range 15-100 nm, penetrating a cancer tumour [10,11]. By penetrating a cancer tumour, from inside the body there may be no need for surgery or heavy chemotherapy in the future. Furthermore, there are literature examples that show nanomaterials, from 10 nm and 15 nm respectively, being detected in rodents brains[12,13]. These examples show the significance of the development of size-controlled nanogels for biomedical applications.

1.2 Size controlled nanogels

1.2.1 Single chain nanoparticles

As mentioned earlier, nanogels have a wide range of opportunities to function in the biomedical sector. Single-chain nanoparticles (SCNPs) are one of these kind of nanogels, which are based on individual crosslinking polymer chains and have a size range up to 20 nm[9]. Due to the small size of these crosslinking nanogels, they can be detected in rodents brains[12,13]. For entering the human body nanogels must be hydrophilic and biocompatible[14]. Literature shows that these SCNPs can be produced hydrophilic and biocompatible. Furthermore, has these SCNPs already show cellular uptake and delivering drugs inside the cell. However, this has only taken place with nanogels up to 20 nm in size. So the ultimate aim is to make the same nanogels with the capacity to be hydrophilic and to being able to attach almost every to it, but with a larger size. If it can be managed to get the chemical structure and function of the nanogels the same for each controlled size. Then size is the only parameter that changes and would it be possible to quantify how size affects, for example, uptake, drug delivery and imaging.

1.2.2 Controlled polymerization techniques

For synthesising nanogels above the size for 20 nm, there are a few radical polymerization techniques that can be used, such as; Atom transfer radical polymerization (ATRP), Reversible addition fragmentation chain transfer (RAFT) and Nitroxide mediated polymerization (NMP)[15][16].

- ATRP:
  Atom transfer radical polymerization is based on the well-established method of carbon-carbon bond formation by atom transfer radical addition used in organic synthesis. A successful ATRP reaction depends on the reversible activation of a dormant species, such as an alkyl halide, by transition of a metal halide catalyst. The metal halide catalyst abstracts the halogen atom from the dormant species to form a radical and an oxidized metal complex[16].

- RAFT:
  RAFT polymerization makes use of a compound that can act as a reversible chain transfer agent[17]. This compound is often a thiocarbonylthio compound. The R' group initiates most polymer chains while the R group stabilizes the intermediate radical species, since this technique promotes the formation of uniform polymer chains in a controlled manner with a low polydispersity.
- *NMP:*
  Nitroxide mediated polymerization is a method of radical polymerization that makes use of a nitroxide initiator to generate polymers with well controlled stereochemistry and a low polydispersity. NMP is based on the use of stable nitroxide radicals mainly 2,2,6,6-tetramethylpiperidine-N-oxyl (TEMPO) and is limited to only a few monomers (styrene derivatives, N,N-dimethylacrylamides, dienes, acrylonitriles). In addition, the process only works satisfactory at higher temperatures (120 to 150 °C) and requires long polymerization times [18].

1.2.3 RAFT Polymerization

In this thesis RAFT-polymerization is used to achieve size-controlled nanogels, since this technique promotes the formation of uniform polymer chains with a low polydispersity in a controlled manner and is also applicable to various monomers, in contrast to NMP. Moreover, RAFT does not require the use of possible toxic metallic initiators, as is the case with ATRP.

RAFT polymerization makes use of a chain-transfer agent in the form of a thiocarbonylthio compound[17], see Figure 1. The R' group initiates most polymer chains and the R group stabilizes the intermediate radical species.

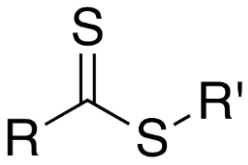

Figure 1: Structure of thiocarbonyl`thio

The components[17,19] used in RAFT polymerization are invariable; A initiator will be used to generate a radical. In general the concentration of this initiator will be very low, while a lower concentration of radicals helps the polymerization to be more "living" by eliminutesating the chances of terminutesation events to occur. A RAFT Agent will be chosen based on the type of monomer and crosslinker in the reaction. Due to RAFT polymerization there is a wide variety of monomers and crosslinkers that can be used. A solvent can be used to slow down the polymerizations rate.

The mechanism of RAFT polymerization involves [15–17,19]; initiation, RAFT Pre-equilibrium, re-initiation, RAFT Main-equilibrium, equilibration and termination, see Figure 2 [17]:

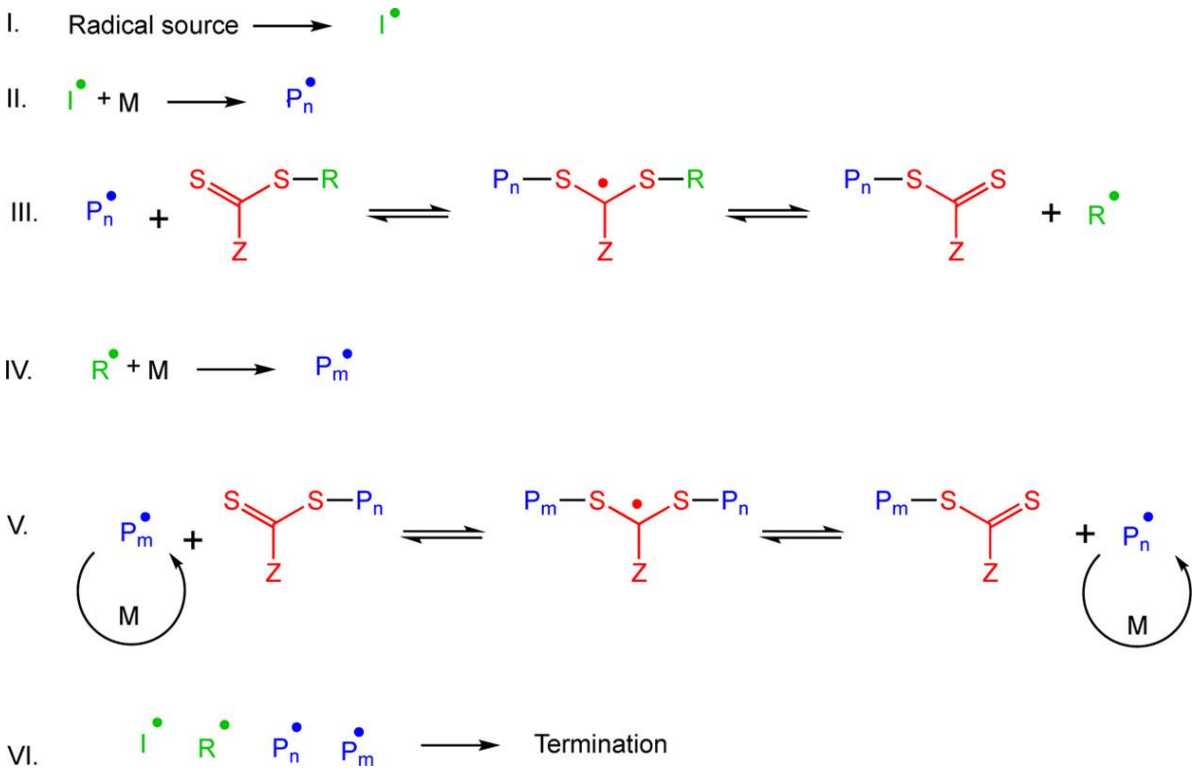

Figure 2: Mechanism of RAFT polymerization

I. Initiation: A small amount of initiator creates some radical species, I^o.

II. Initiation: These radical species will polymerize a small amount of monomer or crosslinker, M. Due to this polymerization a few growing polymer chains will be formed, P_n^o.

III. RAFT Pre-equilibrium: One of the initial polymer chains with an active radical species, Pn^o, will react with the RAFT agent. The radical will combine with an electron from the double bond and forms the intermediate RAFT product. This intermediate RAFT adduct is also a radical, where a Z-group helps stabilizing the intermediate adduct. Next, the radical will form a double bond on the opposite site and kick off the R-group, which creates a new thiocarbonyl. This forms a polymer chain attachment to the RAFT agent and a radical R-group.

IV. Re-initiation: The R-group of the RAFT agent will initiate the grow of new polymer chains. For this step is it important that the concentration of the initiator is low. Due to the low concentration of the initiator, most of the polymer chains that will be generated are initiated by a R-group of the RAFT agent.

V. RAFT main equilibrium: This is the most important part in the RAFT polymerization, where growing polymer chains reversibly attach and detach from the RAFT agent. If a polymer is not attached to the RAFT agent, it is free to undergo further polymerizations with free monomers to grow further. When attached to the RAFT agent, an intermediate radical species is formed. This intermediate radical species has two dormant polymer chains, resulting in equally spread out radicals across all polymer chains. This technique promotes the formation of uniform particles in a controlled manner with a low polydispersity.

VI. Termination: In this step remaining radical species (I^o ,R^o and Pn^o) will react through a bi-radical termination to form chains that cannot react any further.

1.3 Research plan

To achieve size-controlled nanogels with RAFT-polymerization; methyl methacrylate(MMA) as a monomer; Ethylene glycol dimethylacrylate (EGDMA) as a crosslinker, 4-((((2-carboxyethyl)thio)carbonothioyl)thio)-4-cyanopentanoic acid as a RAFT agent and AIBN will be used in the process, see Figure 3.

Using the above described RAFT polymerization components, there are different parameters to achieve the size-controlled nanogels, namely; temperature, reactant concentration and presence of a catalyst[20].

By chancing the temperature of the reaction, the reaction rate can be slowed down or be speeded up. A higher temperature might lead to a faster forming of nanogels.

The reactant concentrations will also affect the size of the nanogels. When changing the concentration of solvent, there will be an effect on the growing speed of the nanogels. A high concentration of solvent will result in a slow downed polymerization rate[21].

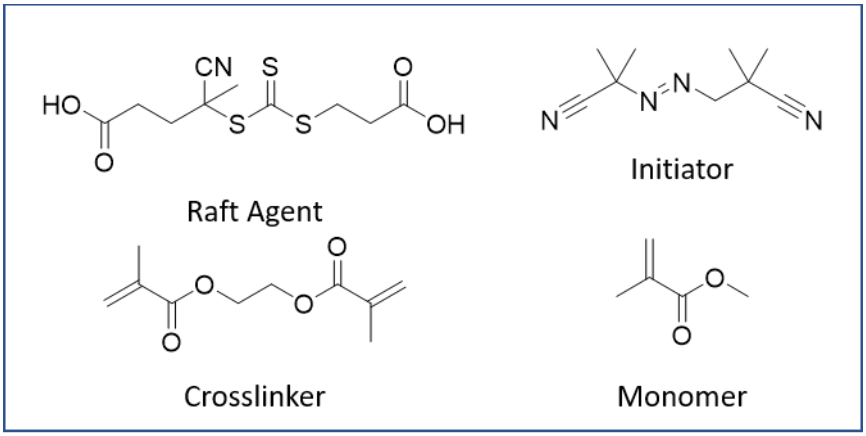

Figure 3: f.l.t.r: MMA, EGDMA, RAFT Agent and AIBN

The presence of a catalyst, is in this case AIBN. AIBN is applied as the initiator and starter of the RAFT polymerization. As mentioned earlier, the initiator will create some radical species, which will polymerize a small amount of monomer or crosslinker. So changing the concentration of the so called initiator, results into two possible outcomes. Adding a small concentration of AIBN to the reaction, leads to a small concentration of radical species. A small concentration of radical species leads to a small amount of polymerized monomer or crosslinker[22]. Due to the small concentration it can be difficult for an active radical species to find a RAFT agent to react with, which can lead to smaller nanogels.

Adding a large concentration of AIBN to the reaction, leads to a large concentration of radical species. This large amount leads to large amount of polymerized monomer or crosslinker[22]. A higher amount of polymerized monomer or crosslinker can lead to earlier termination in the reaction. Earlier termination leads to a smaller size of nanogels.

The aim is to make size-controlled nanogels with the use RAFT polymerization and alterations of the mentioned parameters.

2. Experimental

2.1 Materials

2,2′-Azobis(2-methylpropionitrile) (AIBN), methyl methacrylate(MMA), Ethylene glycol dimethylacrylate (EGDMA), azobisisobutyronitrile (AIBN), 2-cyano-2-propyl benzodithioate, 4-((((2-carboxyethyl)thio)carbonothioyl)thio)-4-cyanopentanoic acid, 1,4-dioxane, heptane, dichloromethane (DCM), dimethylformamide (DMF), chloroform and dimethylsulfoxide were purchased from Sigma-Aldrich. All liquid monomer and crosslinker were passed through a column of Al_2O_3 to remove the inhibitor prior to use.

2.2 Characterization

Nuclear magnetic resonance (NMR) spectra were collected on a Bruker 400 MHz spectrometer. Chemical shifts were reported using the solvent residue as the reference. Dynamic light scattering (DLS) was performed on a Zetasizer Malvern. The size of the nanogel and polydispersity were automatically analysed using ZS Explorer software. Gel permeation chromatography (GPC) was performed on a waters e2695 system, which is equipped with a PLgel 10um MXED-D 300x7.5 mm column. Detection has been performed on refractive index (RI) and photodiode array (PDA) detectors using DMF as the eluent at a flow rate of 0.7 mL/minutes. The temperature of the column was set at 35 °C.

2.3 Synthesis of nanogel

MMA-EGDMA nanogel formation. RAFT Agent 4-((((2-carboxyethyl)thio)carbonothioyl)thio)-4-cyanopentanoic acid (51.03 mg , 0.17 mmol, 0.1 equiv.), AIBN (5.45 mg, 0.03 mmol, 0.02 equiv.), MMA (500 mg, 4.99 mmol, 3 equiv.), EGDMA(329.05 mg, 1.66 mmol, 1 equiv.) and 1,4-dioxane (7.22 ml, 10 wt%) were added to a 25 ml round bottle flask equipped with a stir bar, sealed with a septum and purged with nitrogen for 30 minutes. After purging, the solution was divided into 6, 5 ml round bottle flasks, equipped with a stir bar, sealed with a septum. These 5 ml round bottle flasks were all purged with nitrogen for 15 minutes, to remove all oxygen. Subsequently the 6 flasks were placed in an oil bath at 70°C and allowed to react. After reacting for 2h, the flasks were taken out of the oil bath with a time interval of 10 minutes and put into an ice bath and opened to air to stop the reaction. The nanogels were precipitated in hexane yielding a yellow solid.

MMA-EGDMA ampoules nanogel formation. RAFT Agent 4-((((2-c arboxyethyl)thio) carbonothioyl)thio)-4-cyanopentanoic acid (71.64 mg , 0.233 mmol, 0.1 equiv.), AIBN (7.65mg, 0.04 mmol, 0.02 equiv.), MMA (700 mg, 6.99 mmol, 3 equiv.), EGDMA(461.95 mg, 2.33 mmol, 1 equiv.) and 1,4-dioxane (14.93 ml, 7 wt%) were added to a 50 ml round bottle flask equipped with a stir bar, sealed with a septum and purged with nitrogen for 30 minutes. After purging, the solution was divided into 17, 2 ml ampoules, equipped with a stir bar. After dividing the ampoules they were held in liquid nitrogen for 30 sec, then vacuumed for 30 sec. After the solution had liquefied, this procedure was repeated twice, to ensure that all oxygen had been removed. Subsequently the 17 ampoules were placed in an oil bath at 70°C and allowed to react. After reacting for 95minutes, the flasks were taken out of the oil bath with a time interval of 15 minutes and put into an ice bath and opened to air to stop the reaction. The nanogels were precipitated in hexane yielding a yellow solid.

MMA-EGDMA bulk gel formation. RAFT Agent 4-((((2-carboxyethyl)thio)carbonothioyl)thio)-4-cyanopentanoic acid (13.64 mg , 0.04 mmol, 0.1 equiv.), AIBN (1.45 mg, 0.008 mmol, 0.02 equiv.), MMA (133.53 mg, 1.33 mmol, 3 equiv.), EGDMA(88.12 mg, 0.44 mmol, 1 equiv.) and 1,4-dioxane (0.21 ml, 46.7 wt%) were added to a 5 ml round bottle flask equipped with a stir bar, sealed with a septum and purged with nitrogen for 30 minutes. Subsequently the flask was placed in an oil bath at 70°C and allowed to react. Every 5 minutes the solution was checked, to see if a gelation had formed. After gelation the flask were put into an ice bath and opened to air to stop the reaction. See Appendix 1, for the table with the other concentrations of the gelation reactions.

3. Results and Discussion

MMA-EGDMA nanogels were prepared using RAFT polymerization of methyl methacrylate(MMA) and ethylene glycol dimethacrylate (EGDMA) in a 3:1 mole ratio under dilute conditions, see Figure 4.

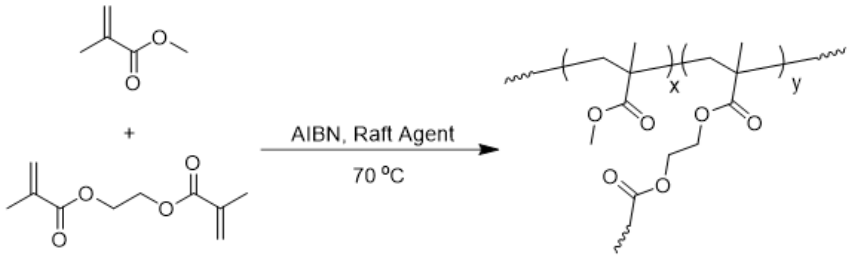

Figure 4: RAFT polymerization of MMA with EGDMA forming MMA-EGDMA nanogels.

3.1 RAFT Agent and AIBN

A RAFT polymerization between a monomer and crosslinker should lead to a gelation in a certain time interval. After this time interval the solution will not be a nanogel anymore, but a macrogel will be formed.

The monomer conversion was determined by H NMR spectroscopy. This have been done by integrating the characteristic signals of the alkene group located at 6.1 and 5.7 ppm. The nanogel size have been determined using dynamic light scattering(DLS), Table 1 shows the size and conversion of these nanogels.

Table 1: Reaction time, size and monomer conversion of the first reactions.

Time (minutes)	Size (nm)	Monomer conversion (%)
120	2.0	14
120	1.5	13
240	2.5	34
480	4.5	54
1440	7.1	71

Table 1 shows the results of the first reactions, the size is increasing with the time, but it did not form a gelation. The conversion on the other hand is increasing as it should be. This means that the amount of the alkene group of the monomer is decreasing.

Therefore another RAFT Agent has been used, to check if a different RAFT agent was forming a gelation after a reaction time of 1020 minutes. RAFT agents are specific for their corresponding monomer[16,23].

Figure 5 present the unprecipitated nanogel solution with RAFT Agent (2-Cyano-2-propyl benzodithioate). As mentioned above, the first reaction did not form a gelation after 24 hours of reaction.

Figure 5: unprecipitated nanogel with RAFT Agent (2-cyano-2-propyl benzodithioate) in hexane.

Unfortunately the other RAFT Agent, did not lead to forming a nanogel at all, with a conversion of 7.75 % after a reaction time of 1020 minutes. The difference in RAFT Agent is in the classes of RAFT agent. On the first hand a trithiocarbonates group was used to form the nanogel, when this did not work a dithiobenzoates group was used to make a nanogel. Unfortunately the dithiobenzoates did not form nanogels at all. This is because the dithiobenzoates group is not most appropriate RAFT agent for methacrylates[24].

After a different RAFT Agent was also not forming a gelation after a certain time. There have been looked to the initiator, AIBN. If the initiator is not working good, there cannot be formed radicals on the RAFT Agent and there will never occur a gelation. So, there have been made a H NMR of AIBN dissolved in chloroform, see Appendix 2. As it can be seen, the spectra at the top gives two peaks around 5.8 ppm. This spectra gives two more peaks than AIBN should give, so the AIBN was decomposed.

In order to get better working AIBN it was recrystallized. This recrystallization has been done by dissolving the AIBN in methanol, and afterward evaporate the methanol with the contamination[25]. To control if the AIBN have been crystallized correctly, there have been made a other H NMR sample, see Appendix 2. As it can be seen the peaks are completely gone after the crystallization process. AIBN has probably decomposed as it has reached a temperature above 30°C[26]. This could easily happen when it is not stored back into the fridge after using it. Due to this decomposed AIBN, it would never be able for MMA-EGDMA solution to form a MMA-EGDMA crosslinked gelation. Due to AIBN being the initiator in the reaction and its property to initiate the polymerization

3.2 Gelation time nanogels

After finding the cause of the not occurring nanogel gelation's after a long time of reaction time. The concentration of the MMA-EGDMA in the solution have been changed. From 7 and 10 wt% it was increased significantly to see after which time a gelation is formed at a certain wt%. These data are plotted in the table, see Table 2.

Table 2: gelation time with different wt%.

Wt%	Gelation time (minutes)
46%	55
38%	85
32%	95
25%	190

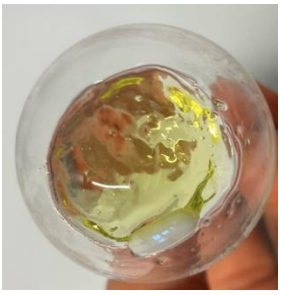

As it can be seen in table 2 the gelation time is decreasing with a decrease of wt%. This is also another confirmation that the recrystallization of AIBN have served its purpose. After this result there is the possibility to change in the wt% in order to get size-controlled nanogels, but by increasing the wt% this significant, it became unstable. The instability of this gelation, it is thought, is because of the increasing wt%[27,28]. A higher wt% means a lower amount of solvent in the reaction. During the "main" reaction, a lot of different reactions takes place; polymerization of the polymer chain, this can be building in series of monomer followed by a crosslinker; or a crosslink between two monomer-crosslink chains; or attaching and detaching from the RAFT Agent; and initiating new polymer chains.

This means that a crosslink between two chains leads to a doubling of the size of the nanogel. If this doubling takes place between two already large chains, this can result in a gelation. From experience during several reactions, with 15-20 wt%. It turned out that it was very difficult to find the right spot to stop a reaction, or to take out samples for smaller sizes nanogels. Further experiments has been done using a lower wt%, but the wt% can certainly play a role in making the size controlled nanogels. However, this is something for future research.

3.3 Different DLS solvents

After being able to make nanogel gelation's at different wt%, we started looking at which solvent gives the best and most stable result in the DLS. Figure 6 presents three different solvents used to analyse the

size of the nanogels, all these measurements were obtained with the same reaction to nanogel. Acetone, DCM and THF solvents were chosen, because of their ability to dissolve MMA-EGDMA nanogels.

As it can be seen above in figure 6, all the solvents gives the results which were expected. Acetone,

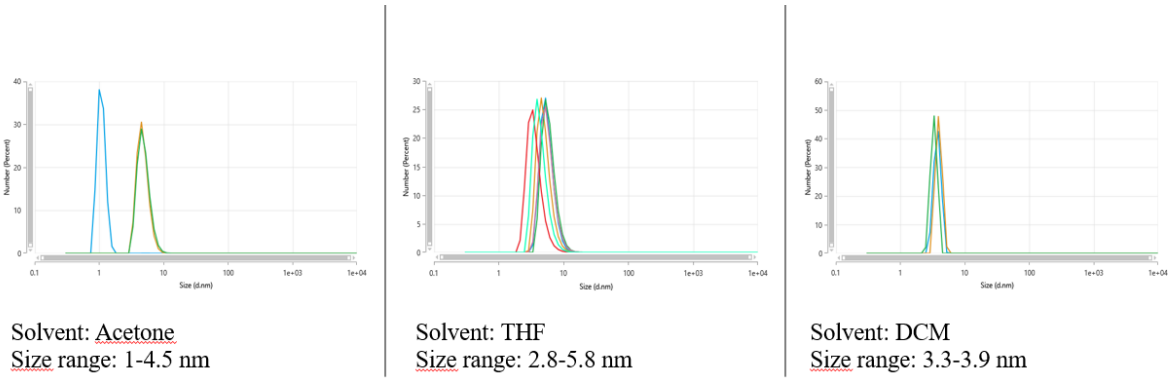

Solvent: Acetone
Size range: 1-4.5 nm

Solvent: THF
Size range: 2.8-5.8 nm

Solvent: DCM
Size range: 3.3-3.9 nm

Figure 6: 3 different DLS solvents, with their size range.

DCM and THF are organic solvents, due to that they have the ability dissolve MMA-EGDMA nanogels. But the different solvents gives some differences; acetone gives a measurement with two peaks. This can be due to a bad measurement or due to acetone making the nanogel unstable. DCM and THF gives stable measurements, but the peaks with THF as solvent are broader than those with DCM. Due to this observation, from now on DLS is only measured with DCM.

3.4 Synthesis nanogels

The ampoules were used to set-up a long reaction time ratio. This has been done with a 7 wt%. The aim was to start from 95 minutes reaction time and take out a sample every 15 minutes to see the grow of the nanogels. This should make it possible to see a growth in the NG over time. Figures 7 & 8

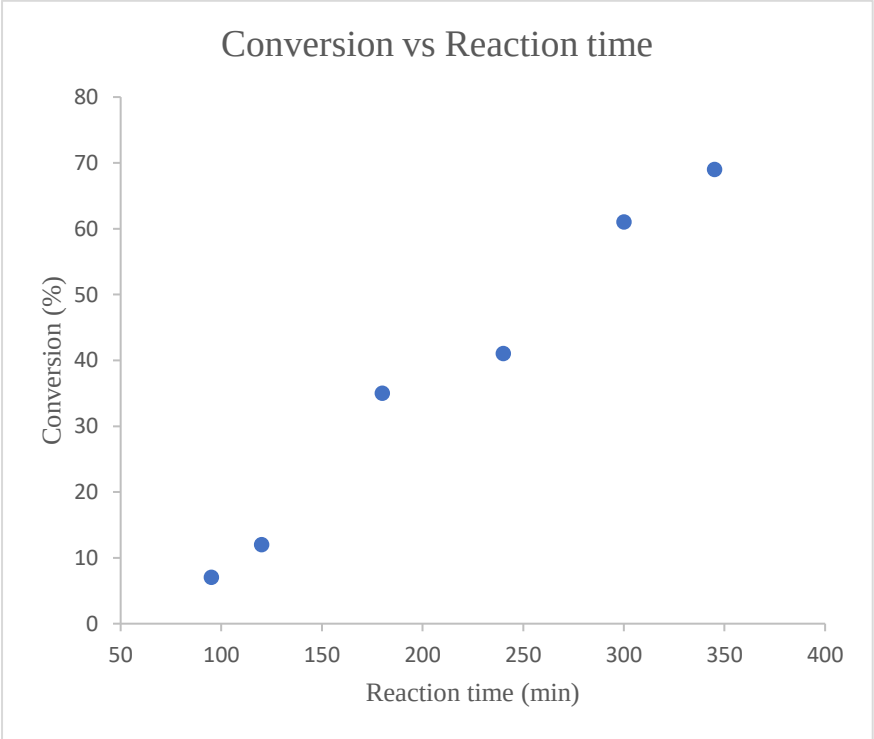

Figure 7: Conversion plotted against reaction time using ampoules.

presents graphs of the nanogel forming using the ampoules technique. Figure 7 shows the monomer conversion against the reaction time, as it can be seen the conversion is increasing against time. Furthermore, the conversion rate increases in a linear relationship, which also fits this graph.

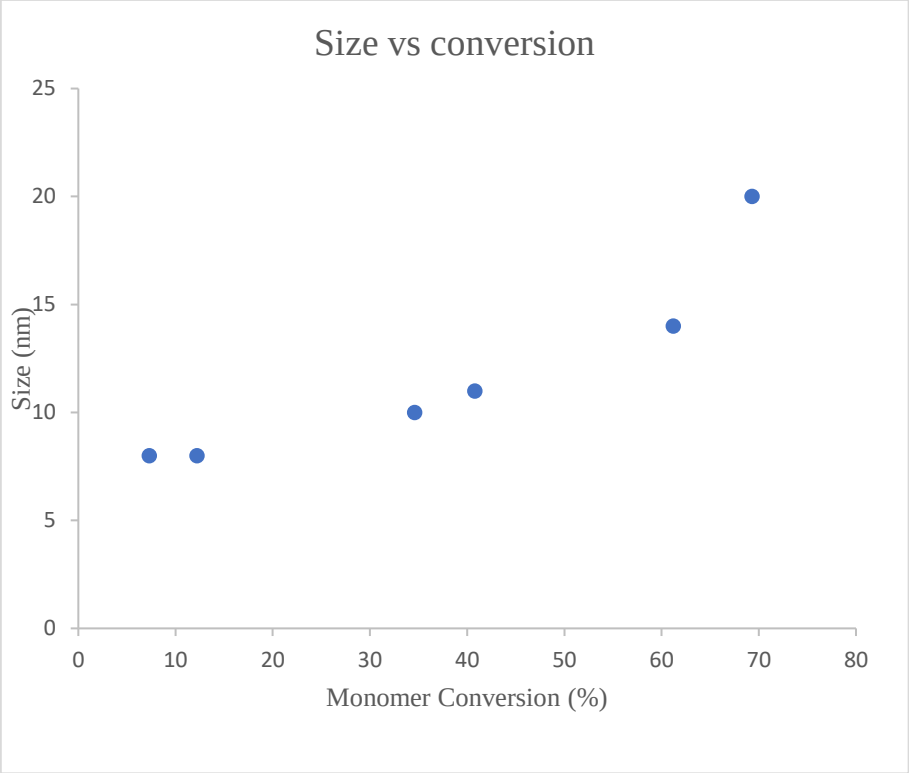

Figure 8: Size as function of monomer conversion.

Figure 8 shows the size of the nanogels against the monomer conversion. The monomer conversion, as is shown in figure 7, gives a normal result over time. Only the size lags behind with the conversion over time. The graph shows indeed a growth in the size of the nanogels. The last two points in the graph indicate that the growth of the nanogels is still going on. Therefore, another experiment was done, to look if the growth continues over a longer period of time. The exact same conditions had been used to check if a gelation would form after an overnight reaction. As mentioned earlier a gelation of the nanogels indicates big sized nanogels[27,28]. However, after the overnight reaction the solution still did not form a gelation and gives a size with DLS of 21 nm. This suggests that the technique with ampoules does not serves its purpose. On the other hand, the conversion of the overnight reaction was 71% calculated using the H NMR spectra. This indicates that a polymer chain from MMA monomers was forming, since the conversion is calculated on the reduction of the area under the peaks, see Appendix 4.

Vacuuming the solution in advance, should have ensured that all the oxygen was removed from the solution. This is necessary, because the oxygen influences the working of the radicals in the polymerization. The present oxygen can react with active radical and generate dead chain ends[29]. Due to reacting with active radicals, the RAFT Agent in the solution cannot act as reversible transfer chains[30]. Due to this it is plausible that the presence of a small amount of oxygen only caused the formation PMMA chains, instead of MMA-EGDMA nanogels. So from here on no more use was made of ampoules.

MMA-EGDMA nanogels were prepared by RAFT polymerization, with the use of round bottom flasks instead of ampoules. After several reactions to get to the gelation, with this type of reactions. Again, a time interval has been set up to achieve size-controlled nanogels. During these reaction every 10 minutes a reaction has stopped. From these sample conversion and size has been determined.

The conversion of the nanogels was calculated through the use of H NMR spectra. Figure 9 shows the combined spectra of 0 minutes and 170 minutes of reaction time, see Appendix 4 for the whole H NMR spectra of the nanogels. The conversion is calculated by integrating the characteristic signals of the alkene group located at 6.1 and 5.7 ppm, and scaling these against the peak around 3.6 ppm, which belongs to 1,4-dioxane. These double are used in the polymerization of the monomers and crosslinker. So a increasing conversion means decreasing in the amount of double bonds in the solution. Furthermore, does this mean that a increase of conversion against reaction time, results in a polymerization of the monomer and crosslinker in the solution.

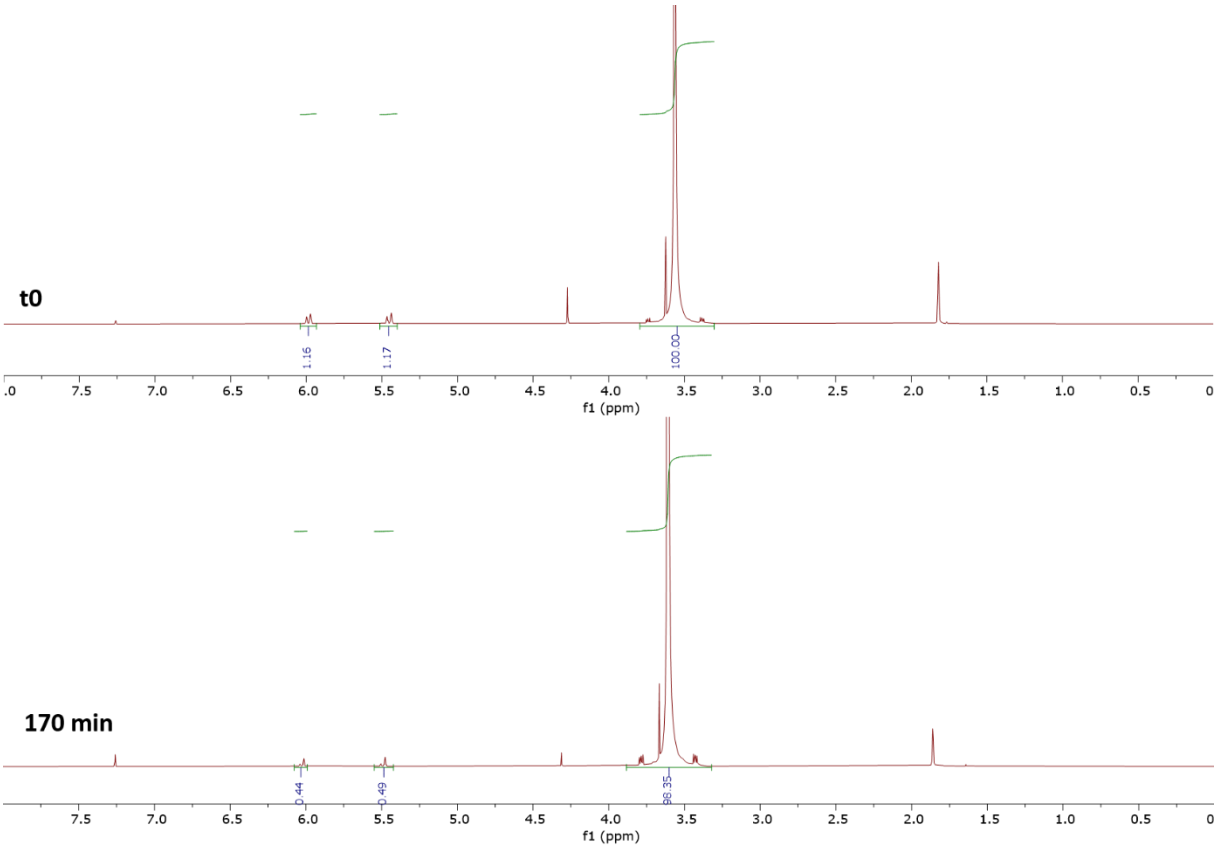

Figure 9: H NMR spectra before reaction and after 170 minutes of reaction time.

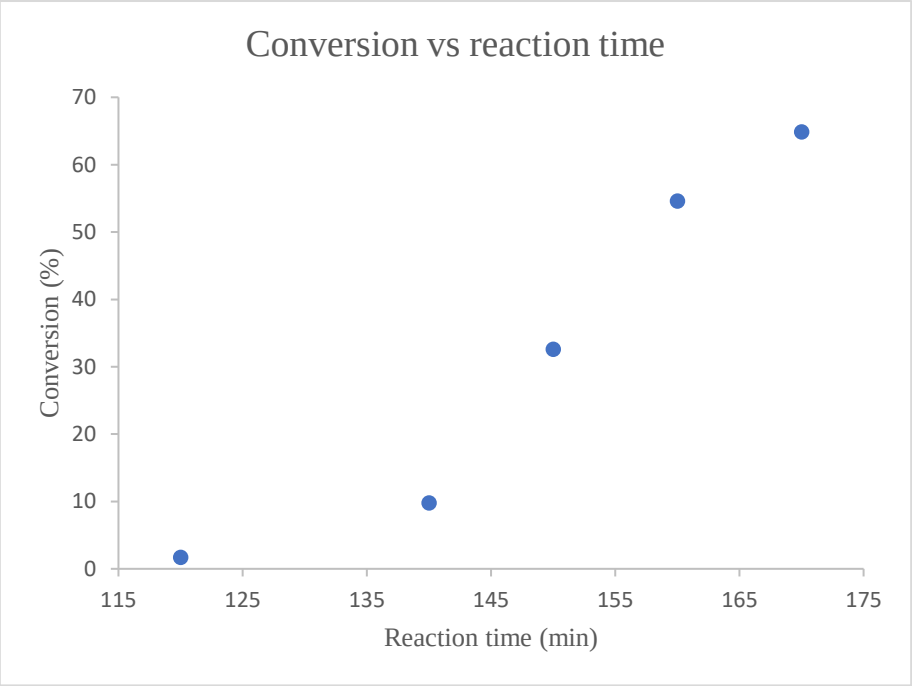

Figure 10: Conversion plotted against reaction time.

Figure 10 shows the monomer conversion against the reaction time, as it can be seen the conversion is increasing against time. Furthermore, the conversion rate increases in a linear relationship, which also fits this graph.

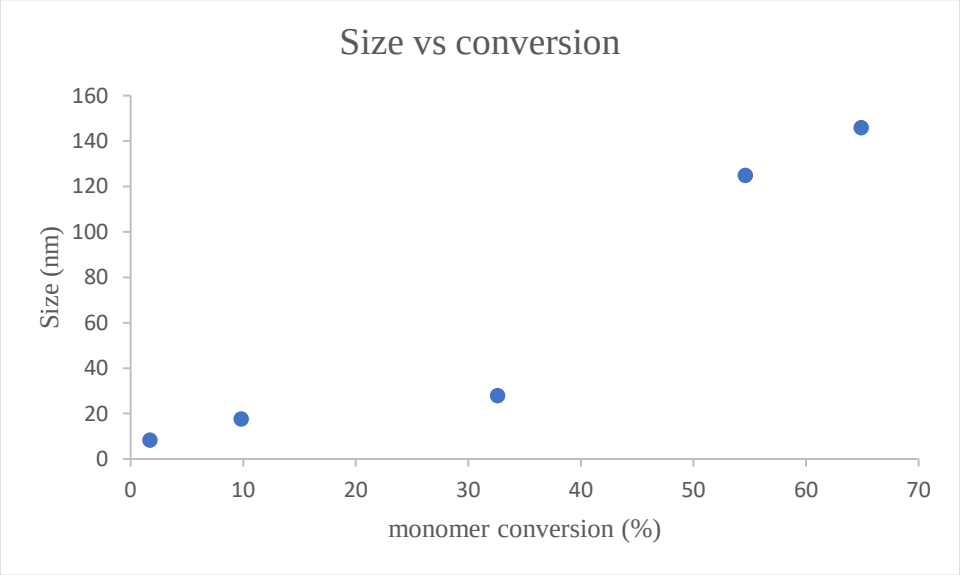

Figure 11: Size as function of monomer conversion.

Figure 11 shows the size plotted against the monomer conversion. If both figures are compared with each other, it can been seen that there is correlation in time against the size of the nanogels. So there is a range built up in size of the nanogels, this range goes from 8 till 146 nm. To validate the DLS results, a GPC experiment was done.

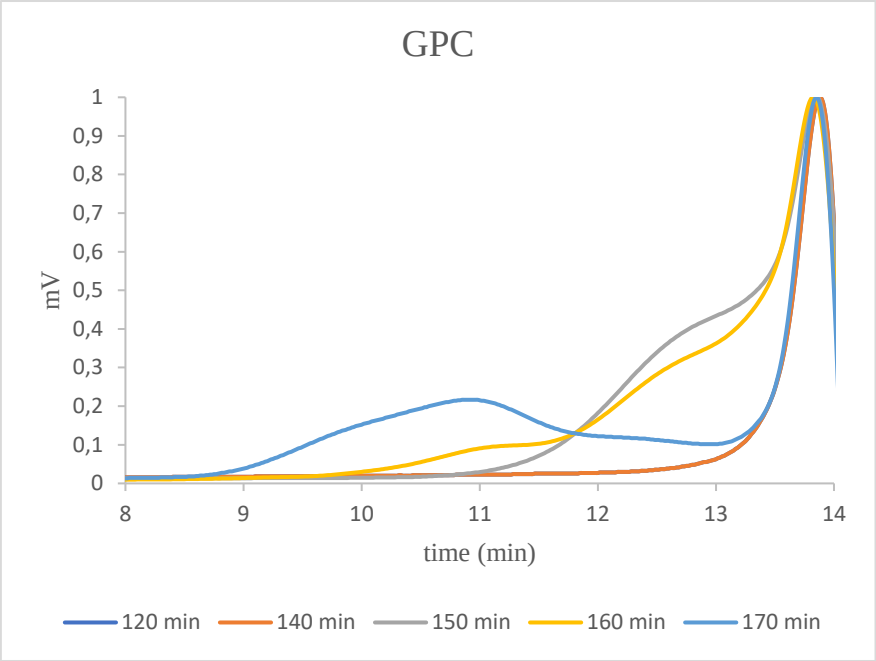

Figure 12: MMA-EGDMA nanogel by GPC.

Figure 12 shows the GPC data of the above showed graph, figure 11. GPC was used to check and confirm the DLS data. Figure 12 does show difference in the size of the nanogels. But it is not exactly correlation to the DLS data. The 170 minutes line should correlate to a size of 146 nm. If this is the case the 160 minutes line does not correlate to a size of 125 nm, but to a smaller size. But it can be more likely that the biggest size nanogel somehow did undergo a formation to bulk gel.

Furthermore, the GPC data shows a broader division of different sizes. This can be seen through the broad peaks of the samples 150, 160 and 170 minutes. One reason may be the way DLS is measured.

The DLS measurement gives data, which is obtained using the number plot of the data. This method scales everything down to the most common size[31]. Using this number distributions the DLS gives just one peak. If the intensity distribution is used, there form 2 peaks. This indicates that there are several nanogels with a different size, which also can be related back to the GPC data. That is also giving a broad division in the peaks. From here, there is concluded that the sizes given by DLS number distribution, are the ones given in the range, so from 8-146 nm. This is done because the number distribution gives the size which is the most common. But as mentioned earlier, it is once shown again that there are many different reactions going on during one “main” reaction. Which makes it really difficult to synthesis size-controlled nanogels.

3.5 Future research

After the synthesis of size-controlled MMA-EGDMA nanogels, there are a few new research goals. The first one is making the nanogels hydrophilic instead of hydrophobic, like the MMA-EGDMA nanogels. Due to the presence of the MMA in the gel, it can never be used in biomedical applications. For that it needs to be hydrophilic, because the more hydrophilic a nanogel is, the less absorption there will be in the body[32]. So for targeted drug delivery or imaging, the nanogel has to get to the specific place of interest. Therefore it needs to have as less absorption as possible.

For making the nanogels hydrophilic the monomer MMA can be changed with Penta fluorophenyl methacrylate(PFMA)[18]. After PFMA is built into the structure, it can be functionalized with solubilizing groups. This will make the outside area of the nanogel hydrophilic, which causes a better transportation through the human body. After making the nanogels hydrophilic, there can also be looked

into attaching a fluorescent dye to it. By doing so, the nanogel can be followed through the body besides which it will be possible to check in which component of the cell the uptake takes place.

Furthermore there can also be future research in changing the concentrations of the components in the RAFT polymerization. This may include changing the monomer-crosslinker ratio from 3:1 to 2:1 or 4:1. Furthermore, changing the wt% of the solvent in the solution also might give, some new insight in the growing of the nanogels. Changing the wt% might let to forming a faster gelation of the nanogels[21]. Therefore, it also might give a different approach to making size-controlled nanogels. Future research will have to show whether this will have an influence

Eventually a small nanogel size range is achieved. However, more data points are needed to call it a real range. Future research should achieve this.

4. Conclusion

MMA-EGDMA nanogels can be synthesized using RAFT polymerization, in a range between 8 - 146 nm. The many reactions to get to this range, show that the method is quite sensitive and needs some finetuning. In the special case, working in fully nitrogen environment, because oxygen was the reason quite some reactions did not work at all. Nevertheless, the first results provide a good start for being able to make and produce size controlled nanogels. However, there is still much work to be done. This work serves to further research in making the nanogels hydrophilic and post functionalize them. When this can be done to the size controlled nanogels, they can be used as a future biomedical application.

5. Acknowledgments

I want to thank the following people for their help and guidance during my thesis.

N. Cengiz, thank you for your daily supervision during my thesis, specifically in giving advice and support during the whole period. During this period I have learned a lot about doing research.

Dr. ir. Jos Paulusse, thank you for hosting me in your research group and giving me the opportunity for doing research in the biomedical sector.

6. Literature

[1] Tsintou M, Wang C, Dalamagkas K, Weng D, Zhang YN, Niu W. Nanogels for biomedical applications: Drug delivery, imaging, tissue engineering, and biosensors. Nanobiomaterials Sci Dev Eval 2017:87–124. https://doi.org/10.1016/B978-0-08-100963-5.00005-7.

[2] Soni KS, Desale SS, Bronich TK. Nanogels: an overview of properties, biomedical applications and obstacles to clinical translation. J Control Release 2016;240:109. https://doi.org/10.1016/J.JCONREL.2015.11.009.

[3] Xu Y, Li Y, Cao X, Chen Q, An Z. Versatile RAFT dispersion polymerization in cononsolvents for the synthesis of thermoresponsive nanogels with controlled composition, functionality and architecture. Polym Chem 2014;5:6244–55. https://doi.org/10.1039/C4PY00867G.

[4] Chan M, Almutairi A. Nanogels as imaging agents for modalities spanning the electromagnetic spectrum. Mater Horizons 2016;3:21. https://doi.org/10.1039/C5MH00161G.

[5] Keskin D, Tromp L, Mergel O, Zu G, Warszawik E, Van Der Mei HC, et al. Highly Efficient Antimicrobial and Antifouling Surface Coatings with Triclosan-Loaded Nanogels. ACS Appl Mater Interfaces 2020;12:57721–31. https://doi.org/10.1021/ACSAMI.0C18172/ASSET/IMAGES/LARGE/AM0C18172_0008.JPEG.

[6] Kadry H, Noorani B, Cucullo L. A blood–brain barrier overview on structure, function, impairment, and biomarkers of integrity. Fluids Barriers CNS 2020 171 2020;17:1–24. https://doi.org/10.1186/S12987-020-00230-3.

[7] Persidsky Y, Ramirez SH, Haorah J, Kanmogne GD. Blood-brain Barrier: Structural Components and Function Under Physiologic and Pathologic Conditions 2006. https://doi.org/10.1007/s11481-006-9025-3.

[8] Liu D, Mori A, Huang L. Role of liposome size and RES blockade in controlling biodistribution and tumor uptake of GM1-containing liposomes. BBA - Biomembr 1992;1104:95–101. https://doi.org/10.1016/0005-2736(92)90136-A.

[9] Kröger APP, Paulusse JMJ. Single-chain polymer nanoparticles in controlled drug delivery and targeted imaging. J Control Release 2018;286:326–47. https://doi.org/10.1016/J.JCONREL.2018.07.041.

[10] Sykes EA, Dai Q, Sarsons CD, Chen J, Rocheleau J V., Hwang DM, et al. Tailoring nanoparticle designs to target cancer based on tumor pathophysiology. Proc Natl Acad Sci U S A 2016;113:E1142–51. https://doi.org/10.1073/PNAS.1521265113.

[11] Zhang F, Trent Magruder J, Lin YA, Crawford TC, Grimm JC, Sciortino CM, et al. Generation-6 hydroxyl PAMAM dendrimers improve CNS penetration from intravenous administration in a large animal brain injury model. J Control Release 2017;249:173–82. https://doi.org/10.1016/J.JCONREL.2017.01.032.

[12] De Jong WH, Hagens WI, Krystek P, Burger MC, Sips AJAM, Geertsma RE. Particle size-dependent organ distribution of gold nanoparticles after intravenous administration. Biomaterials 2008;29:1912–9. https://doi.org/10.1016/J.BIOMATERIALS.2007.12.037.

[13] Sonavane G, Tomoda K, Makino K. Biodistribution of colloidal gold nanoparticles after intravenous administration: Effect of particle size. Colloids Surfaces B Biointerfaces 2008;66:274–80. https://doi.org/10.1016/J.COLSURFB.2008.07.004.

[14] Saarbrücken A-VW. Hydrophilic Drug Delivery based on Gelatin Nanoparticles 2018.

[15] Chen M, Zhong M, Johnson JA. Light-Controlled Radical Polymerization: Mechanisms, Methods, and Applications 2016. https://doi.org/10.1021/acs.chemrev.5b00671.

[16] Cowie JMG, Arrighi V. Polymers: Chemistry and physics of modern materials. third edit. Taylor & Francis group; 2007.

[17] Perrier SS. 50th Anniversary Perspective: RAFT Polymerization□A User Guide. Macromolecules 2017;50. https://doi.org/10.1021/acs.macromol.7b00767.

[18] Eberhardt M, Théato P. RAFT Polymerization of Pentafluorophenyl Methacrylate: Preparation of Reactive Linear Diblock Copolymers a n.d. https://doi.org/10.1002/marc.200500390.

[19] Holmberg AL, Karavolias MG, Epps TH. RAFT polymerization and associated reactivity ratios of methacrylate-functionalized mixed bio-oil constituents. Polym Chem 2015;6:5728–39. https://doi.org/10.1039/C5PY00291E.

[20] Bradley MJ, De La Cruz EM. Analyzing ATP utilization by DEAD-box RNA helicases using kinetic and equilibrium methods. Methods Enzymol 2012;511:29–63. https://doi.org/10.1016/B978-0-12-396546-2.00002-4.

[21] Pan X, Zhang F, Choi B, Luo Y, Guo X, Feng A, et al. Effect of solvents on the RAFT polymerization of N-(2-hydroxypropyl) methacrylamide. Eur Polym J 2019;115:166–72. https://doi.org/10.1016/J.EURPOLYMJ.2019.03.016.

[22] Nogueira TR, GonçAlves MC, Lona LMF, Vivaldo-Lima E, McManus N, Penlidis A. Effect of initiator type and concentration on polymerization rate and molecular weight in the bimolecular

nitroxide-mediated radical polymerization of styrene. Adv Polym Technol 2010;29:11–9. https://doi.org/10.1002/ADV.20170.

[23] Perrier S. 50th Anniversary Perspective: RAFT Polymerization - A User Guide. Macromolecules 2017;50:7433–47. https://doi.org/10.1021/ACS.MACROMOL.7B00767/ASSET/IMAGES/LARGE/MA-2017-00767N_0008.JPEG.

[24] Mayadunne RTA, Rizzardo E, Chiefari J, Chong YK, Moad G, Thang SH. Living Radical Polymerization with Reversible Addition−Fragmentation Chain Transfer (RAFT Polymerization) Using Dithiocarbamates as Chain Transfer Agents. Macromolecules 1999;32:6977–80. https://doi.org/10.1021/MA9906837.

[25] Li YJ, Wu K, Li Y, Zhang Y, Liu JJ, Wang XZ. Solubility in Different Solvents, Crystal Polymorph and Morphology, and Optimization of Crystallization Process of AIBN. J Chem Eng Data 2018;63:27–38. https://doi.org/10.1021/ACS.JCED.7B00538/SUPPL_FILE/JE7B00538_SI_001.PDF.

[26] Guo S, Wan W, Chen C, Chen WH. Thermal decomposition kinetic evaluation and its thermal hazards prediction of AIBN. J Therm Anal Calorim 2013;113:1169–76. https://doi.org/10.1007/S10973-013-2993-7/FIGURES/10.

[27] Sahu P, Kashaw SK, Sau S, Kushwah V, Jain S, Agrawal RK, et al. pH triggered and charge attracted nanogel for simultaneous evaluation of penetration and toxicity against skin cancer: In-vitro and ex-vivo study HHS Public Access. Int J Biol Macromol 2019;128:740–51. https://doi.org/10.1016/j.ijbiomac.2019.01.147.

[28] Pujana MA, Pérez-Álvarez L, Iturbe LCC, Katime I. Water dispersible pH-responsive chitosan nanogels modified with biocompatible crosslinking-agents. Polymer (Guildf) 2012;53:3107–16. https://doi.org/10.1016/J.POLYMER.2012.05.027.

[29] Simič R, Mandal J, Zhang K, Spencer ND. Oxygen inhibition of free-radical polymerization is the dominant mechanism behind the “mold effect” on hydrogels. Soft Matter 2021;17:6394–403. https://doi.org/10.1039/D1SM00395J.

[30] Moad G, Rizzardo E, Thang SH. RAFT Polymerization and Some of its Applications FOCUS REVIEW. Chem Asian J 2013;8:1634–44. https://doi.org/10.1002/asia.201300262.

[31] Farkas N, Kramar JA. Dynamic light scattering distributions by any means. J Nanoparticle Res 2021;23:1–11. https://doi.org/10.1007/S11051-021-05220-6/FIGURES/4.

[32] 4 Factors Affecting Solubility of Drugs | Ascendia Pharmaceuticals n.d. https://ascendiapharma.com/2021/07/05/factors-affecting-drug-solubility/ (accessed 30 June 2022).

7. Appendix

7.1 Appendix 1: MMA-EGDMA gelation reaction

Dilution	RAFT Agent	AIBN	MMA	EGDMA	1,4-dioxane
25 %	17.82 mg, 0.06 mmol, 0.1 equiv.	1.90 mg, 0.01 mmol, 0.02 equiv.	175.46 mg, 1.75 mmol, 3 equiv.	115.79 mg, 0.58mmol, 1 equiv.	0.28 ml
32 %	12.63 mg, 0.04 mmol, 0.1 equiv.	1.35 mg, 0.008 mmol, 0.02 equiv.	123.61 mg, 1.23 mmol, 3 equiv.	81.57 mg, 0.41 mmol, 1 equiv.	0.19
38 %	12.57 mg, 0.04 mmol, 0.1 equiv.	1.34 mg, 0.008mmol, 0.02 equiv.	123.09 mg, 1.23 mmol, 3 equiv.	81.23 mg, 0.41 mmol, 1 equiv.	0.19 ml
46 %	13.64 mg, 0.04 mmol, 0.1 equiv.	1.31 mg, 0.008 mmol, 0.02 equiv.	133.53 mg, 1.33 mmol, 3 equiv.	88.12 mg, 0.44 mmol, 1 equiv.	0.21 l

7.2 Appendix 2: H NMR-Spectra uncrystallized and recrystallized AIBN

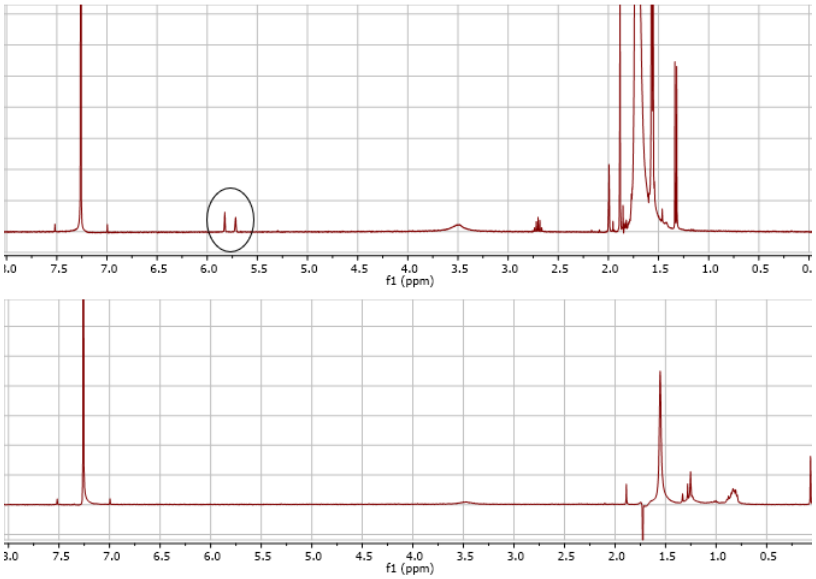

At the top is the uncrystallized AIBN, at the bottom part the recrystallized AIBN.

7.3 Appendix 3: Reaction time, size and monomer conversion reaction ampoules.

Time (minutes)	Size (nm)	Monomer conversion (%)
95	8	7.30
120	8	12.20
180	10	34.60
240	11	40.80
300	14	61.20
345	20	69.30

7.4 Appendix 4: H NMR spectra MMA-EGDMA nanogel

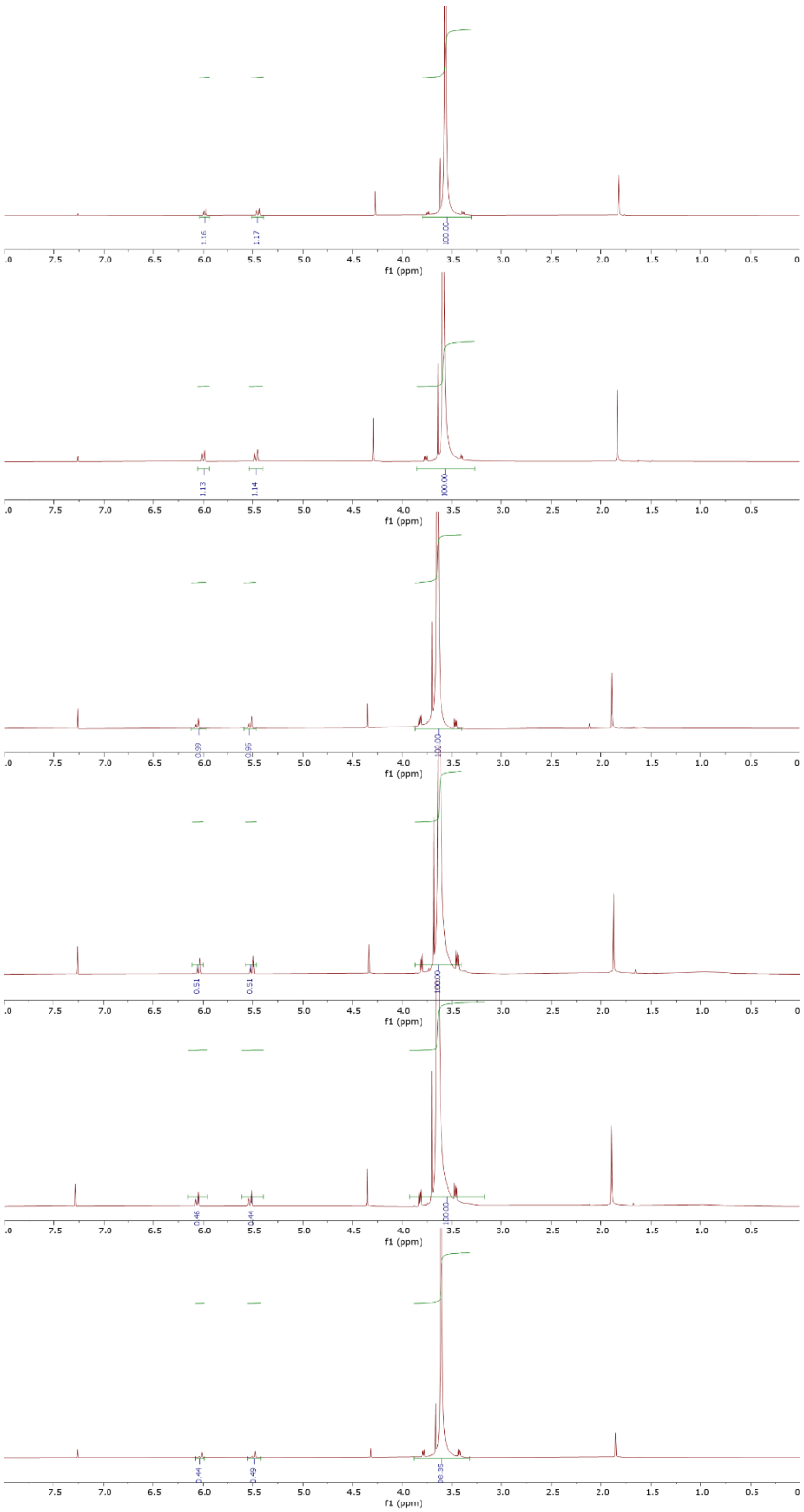

From top to bottom it gives spectra of 0 min, 120 min, 140 min, 150 min, 160 min and 170 min of reaction time, with the integration.